Pergamon

Int. J. Solids Structures Vol. 31, No. 11, pp. 1537–1548, 1994

0020–7683/94 $7.00 + .00

0020–7683(93)E0039–K

COUPLED THERMOELASTIC EFFECTS IN RAPID STEADY-STATE QUASI-BRITTLE FRACTURE

L. M. BROCK
Department of Engineering Mechanics, University of Kentucky, Lexington, KY 40506, U.S.A.

(*Received* 1 *September* 1993; *in revised form* 21 *November* 1993)

Abstract—The steady-state analyses of rapid quasi-brittle fracture generated in both a non-thermal and a fully coupled thermoelastic sheet are performed. Compressive forces moving on both faces of the crack drive the process, and a Dugdale zone represents a rudimentary inelastic region at the crack-edge. For the thermal problem, the region behavior is also characterized by an effective heat flux from the zone. For a given crack speed the loading required, the resulting zone size and, in the thermal study, the heat flux function, are determined from exact solutions by matching typical COD and crack-edge temperature data. Both the thermal and non-thermal studies show a fall-off with increasing crack speed in both the load and zone size. However, the loading and the zone lengths in the two studies differ noticeably. Moreover, the coupled thermoelastic solution is, in general, more sensitive to crack speed.

INTRODUCTION

It is known (Rice and Levy, 1969; Weichert and Schoenert, 1978; Parvin, 1979; Zehnder and Rosakis, 1991) that significant temperature rises can occur during dynamic fracture. Consistent with observations by Taylor and Quinney (1934), these are associated with crack-edge plasticity. In general, dynamic fracture–temperature studies use the uncoupled equations of elasticity (Chadwick, 1960). This simplifies analysis, and is justified by experimental results (e.g. Shockey *et al.*, 1983; Rosakis *et al.*, 1992), which indicate temperature rises confined adiabatically to the crack-edge vicinity, and calculations (e.g. Freund and Hutchinson, 1985) which show that plastic work rate should dominate elastic coupling.

Brock *et al.* (1992), Brock and Thomas (1992) and Brock (1993), hereafter referred to as (B), used a somewhat different approach for rapid quasi-brittle fracture. The material outside a rudimentary inelastic crack-edge zone was allowed to be a fully coupled thermoelastic solid, and the zone itself was characterized by the standard Dugdale (1960) yield model. The zone thermoplastic response was represented by an effective heat flux but, in contrast to similar strip models (Parvin, 1979), the heat flux function was to be determined from the analysis itself.

This approach, which *de facto* views the inelastic zone as a boundary effect, did not require the details of specific thermoplastic models, yet could incorporate experimental data (Brock, 1992a). Transient analyses, exact for short times after fracture initiation, were performed, and gave crack-edge temperature rises that seemed to be approaching values found by Zehnder and Rosakis (1991) in steady-state crack propagation experiments.

In this paper, the representation of (B) is used to gain insight into coupled thermoelastic effects in predicting zone size and the loads necessary to drive rapid, quasi-brittle fracture. This requires an adaptation to the steady-state, because efforts will be made to incorporate experimental data from this type of crack propagation. This adaptation will also allow examination of the representation in a setting quite different from the transient, short-time studies of (B).

To maintain first-step simplicity, an unbounded, linearly thermoelastic, isotropic, homogeneous sheet is treated. A semi-infinite crack is opened in the sheet by equal compressive point forces (line loads across the sheet thickness) which move along the two crack faces. The process is assumed to reach a steady-state in which the crack-edge and forces move at the same constant, subcritical speed. A Dugdale (1960) zone of fixed length is

assumed to form at the crack-edge. The crack propagation satisfies a COD criterion (Ewalds and Wanhill, 1985) and the crack-edge temperature field, like the COD, will be treated as experimentally known.

In the next section, the corresponding non-thermal problem is stated, and some key results given. Subsequently, the thermoelastic problem is stated and solved exactly. Certain aspects of the two solutions are then compared for the insight mentioned above.

NON-THERMAL PROBLEM

Consider the unbounded xy-plane occupied by an elastic sheet. A semi-infinite crack grows along the x-axis. An inelastic zone of constant length d and vanishing thickness has formed ahead of the crack, and the process is driven by two equal compressive forces (line loads in the out-of-plane direction) of magnitude P. As shown schematically in Fig. 1, these forces slide, one on each crack face, without friction, a fixed distance L behind the inelastic zone edge, with $L \geqslant d$. In Fig. 1, c is the crack speed non-dimensionalized with respect to the dilatational wave speed v_1 in the sheet, and is constant and subcritical, i.e.

$$c < c_R < 1/m < 1, \quad m = v_1/v_2. \tag{1}$$

Here (c_R, v_2) are, respectively, the non-dimensionalized Rayleigh wave speed and the rotational wave speed. As also seen in Fig. 1, the origin of the coordinate system is affixed to the moving inelastic zone edge. Then, the problem symmetry about the x-axis and the assumption of a steady-state give the governing equations

$$\nabla^2\mathbf{u} + (m^2-1)\nabla(\nabla\cdot\mathbf{u}) - m^2c^2\mathbf{u}_{,xx} = 0 \tag{2a}$$

$$\frac{1}{\mu}(\sigma_x, \sigma_y) = u_{x,x}(m^2, m^2-2) + u_{y,y}(m^2-2, m^2) \tag{2b}$$

$$\frac{1}{\mu}\sigma_{xy} = u_{x,y} + u_{y,x} \tag{2c}$$

for $y > 0$, and

$$\sigma_{xy} = 0, \quad u_y = 0 (x > 0), \quad \sigma_y = -P\delta(x+L) + YH(x+d) \quad (x < 0) \tag{3}$$

along $y = 0^+$, where (∇^2, ∇) are the two-dimensional Laplacian and gradient operators, $\mathbf{u} = \mathbf{u}(x, y)$ is the displacement with (x, y)-components (u_x, y_y), and $(\cdot)_{,i}$ denotes i-differentiation. Here (δ, H) are the Dirac delta and Heaviside functions, and (μ, Y) are the shear modulus and yield stress. The field $\mathbf{u}$ is bounded as $\sqrt{(x^2+y^2)} \to \infty$ and continuous everywhere.

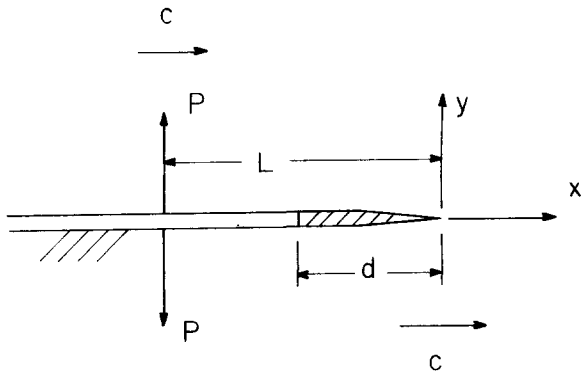

Fig. 1. Schematic of rapid quasi-brittle fracture.

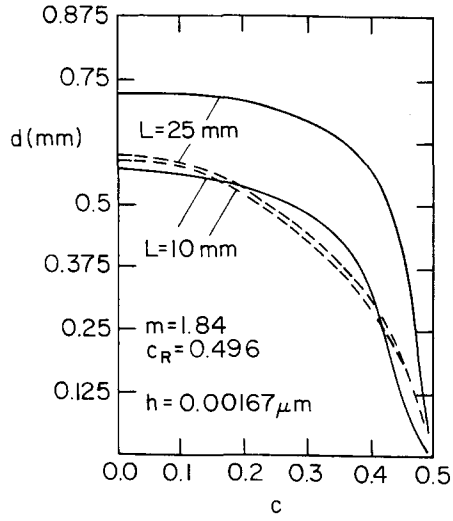

Fig. 2. Zone length d vs non-dimensionalized crack speed c for non-thermal (---) and thermal (——) cases.

This mixed boundary-value problem can be easily solved by a variety of methods similar to those used in static problems (e.g. Sneddon and Lowengrub, 1969; Freund, 1990). In particular, the normal traction just ahead of the inelastic zone edge ($y = 0$, $x = 0^+$) is obtained as

$$\sigma_y \sim \frac{-1}{\pi\sqrt{x}}\left(2Y\sqrt{d} - \frac{P}{\sqrt{L}}\right). \tag{4}$$

It is noted that the coefficient of the singular term does not depend explicitly on the crack speed (c), a result similar to that seen by Yoffe (1951) for a finite crack moving through the solid under uniform tension. The Dugdale (1960) model precludes singular behavior in any case, so that the relation

$$d = \left(\frac{P}{2Y}\right)^2 \frac{1}{L} \tag{5}$$

must hold. The COD δ_t at the tail of the inelastic zone ($y = 0$, $x = -d$) is also easily obtained as

$$\delta_t = \frac{m^2c^2a}{\mu\pi R}\left[P \ln \sqrt{\left(\frac{\sqrt{L}+\sqrt{d}}{\sqrt{L}-\sqrt{d}}\right)} - 2Yd\right]. \tag{6}$$

Here R is the Rayleigh function, where $R(\pm c_R) = 0$ and

$$R = 4\sqrt{(1-c^2)}\sqrt{(1-m^2c^2)} - K^2, \quad a = \sqrt{(1-c^2)}, \quad K = m^2c^2 - 2. \tag{7}$$

If (δ_t, L) are prescribed, then (5) and (6) can be used to obtain the inelastic zone length d and applied load P associated with a given crack speed parameter c. Plots of (d, P) vs $c < c_R$ are given by the broken lines in Figs 2 and 3, respectively, for the two cases $L = 0.01$ and 0.025 m. For these plots, the material properties

$$\mu = 79.3 \text{ GPa}, \quad Y = 1.58 \text{ GPa}, \quad m = 1.84, \quad \delta_t = 5.52\,\mu\text{m}, \quad c_R = 0.496 \tag{8}$$

corresponding roughly to those for a 4130HT steel are used. The non-dimensionalized Rayleigh wave speed c_R is defined in terms of m by the exact formula (Brock, 1992b)

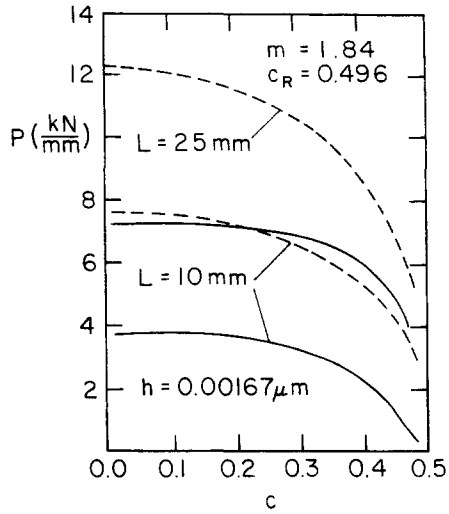

Fig. 3. Load P vs non-dimensionalized crack speed c for non-thermal (---) and thermal (——) cases.

$$m^2 c_R = \sqrt{[2(m^2-1)]}G_0, \quad \ln G_0 = \frac{-1}{\pi}\int_1^m \frac{dt}{t}\tan^{-1}\frac{4t^2\sqrt{(t^2-1)}\sqrt{(m^2-t^2)}}{(m^2-2t^2)^2}. \tag{9}$$

Figures 2 and 3 show that both (d, P) fall off with increasing crack speed. That is, faster crack propagation requires smaller loads, and gives rise to smaller inelastic zones.

Although L is not the parameter of interest here, Figs 2 and 3 do show for a given c that both (d, P) vary directly with it. That is, for a given crack propagation rate, it is more efficient to keep the applied force closer to the zone.

With this preliminary study completed, attention is now focused on the original thermoelastic problem.

THERMOELASTIC PROBLEM: WIENER–HOPF SOLUTION

Consider the same sheet–crack situation of Fig. 1, but now allow the sheet to satisfy the coupled equations of thermoelasticity, and to have an ambient temperature T_0 (K) > 0. Then (2a, b) are replaced by (Chadwick, 1960) the relations

$$\nabla^2\mathbf{u} + (m^2-1)\nabla(\nabla\cdot\mathbf{u}) + \beta\nabla\theta - m^2c^2\mathbf{u}_{,xx} = 0, \quad \beta = \beta_0(4-3m^2) < 0 \tag{10a}$$

$$\frac{k}{\mu}\nabla^2\theta + c_v c\frac{m}{v_2}\theta_{,x} - c\beta T_0 v_1(\nabla\cdot\mathbf{u})_{,x} = 0 \tag{10b}$$

$$\frac{1}{\mu}(\sigma_x, \sigma_y) = u_{x,x}(m^2, m^2-2) + u_{y,y}(m^2-2, m^2) + \beta\theta \tag{10c}$$

for $y > 0$, and to (3) is added the symmetry-based heat flow conditions

$$\theta_{,y} = 0 \quad (x < -d, x > 0), \quad \theta_{,y} = -F(x) \quad (-d < x < 0) \tag{11}$$

along $y = 0^+$. Here θ(K) $= \theta(x, y)$ is the change in temperature from T_0 while (β_0, k, c_v) are, respectively, the coefficient of linear expansion, thermal conductivity and specific heat at constant deformation. In (11) F is the heat flux emanating from the inelastic zone. This quantity characterizes the thermal response of the zone and, for the moment, is arbitrary, save for the requirements that it be bounded and continuous in the interval $-d < x < 0$. In addition, the fields $(\mathbf{u}, \theta)$ should be bounded as $\sqrt{(x^2+y^2)} \to \infty$ and continuous everywhere.

The equation set (2c), (3), (10) and (11) constitutes a mixed boundary-value problem for $y > 0$. The Wiener–Hopf technique (Noble, 1958) will be used to solve the problem, and so the mixed conditions (3) are replaced with

$$\sigma_{xy} = 0, \quad \sigma_y = -P\delta(x+L) + YH(x+d)H(-x) + \sigma_+(x)H(x), \quad u_y = V_-(x)H(-x), \tag{12}$$

where the unknown functions (σ_+, V_-) are introduced to allow all three quantities $(\sigma_{xy}, \sigma_y, u_y)$ to be defined everywhere along $y = 0^+$. The aforementioned continuity of $\mathbf{u}$ demands that

$$V_-(0^-) = 0. \tag{13}$$

Application of the bilateral transform

$$g^* = \int_{-\infty}^{\infty} g(x)\, \mathrm{e}^{-qx}\, \mathrm{d}x, \tag{14}$$

where q is, in general, complex, reduces (10a, b) to a homogeneous, coupled set of ordinary differential equations for $(\mathbf{u}^*, \theta^*)$ in y. Solutions to this set that are bounded for $y > 0$ and the resulting stress transforms are

$$\beta\theta^* = m^2(M_+\bar{A}_+ + M_-\bar{A}_-), \quad \bar{A}_\pm = A_\pm\, \mathrm{e}^{-\alpha_\pm y} \tag{15a}$$

$$u_x^* = -q\bar{A}_+ - q\bar{A}_- + \bar{B}, \quad \bar{B} = B\,\mathrm{e}^{-by} \tag{15b}$$

$$u_y^* = \alpha_+\bar{A}_+ + \alpha_-\bar{A}_- - \frac{q}{b}\bar{B} \tag{15c}$$

$$\frac{1}{\mu}\sigma_{xy}^* = -2q\alpha_+\bar{A}_+ - 2q\alpha_-\bar{A}_- + \frac{T}{b}\bar{B} \tag{15d}$$

$$\frac{1}{\mu}\sigma_y^* = -T\bar{A}_+ - T\bar{A}_- - 2q\bar{B} \tag{15e}$$

$$\frac{1}{\mu}\sigma_x^* = T_+\bar{A}_+ + T_-\bar{A}_- + 2q\bar{B}, \tag{15f}$$

where $(A_\pm, B)$ are arbitrary functions of q and

$$T = Kq^2, \quad T_\pm = 2\alpha_\pm^2 - m^2c^2q^2, \quad b = \sqrt{(1-m^2c^2)}\sqrt{(-q^2)} \tag{16a}$$

$$M_\pm = -cq[(r_+ \pm r_-)^2 + cq], \quad \alpha_\pm = \sqrt{(-cq)}\sqrt{\left[(r_+ \pm r_-)^2 + \frac{q}{c}\right]} \tag{16b}$$

$$2r_\pm = \sqrt{\left[\left(\sqrt{(-cq)} \pm \frac{1}{\sqrt{h}}\right)^2 + \frac{\varepsilon}{h}\right]}. \tag{16c}$$

In (16), (h, ε) are, respectively, a thermoelastic characteristic length and a dimensionless constant defined by

$$h = \frac{kv_2}{\mu c_v m}, \qquad \varepsilon = \frac{T_0}{c_v}\left(v_2\frac{\beta}{m}\right)^2. \tag{17}$$

The latter quantity is the so-called coupling constant, and is generally $O(10^{-2})$ or less

(Chadwick, 1960). It can be shown that both (b, α_-) have the branch cuts $\mathrm{Im}\,(q) = 0$, $|\mathrm{Re}\,(q)| > 0$, while α_+ exhibits the cuts $\mathrm{Im}\,(q) = 0$, $\mathrm{Re}\,(q) > 0$, $\mathrm{Re}\,(q) < -q_\varepsilon$, where

$$hq_\varepsilon = c_\varepsilon = c\left(1+\frac{\varepsilon}{1-c^2}\right). \tag{18}$$

These choices guarantee that $\mathrm{Re}\,(b, \alpha_\pm) \geqslant 0$ in the cut plane. It can be shown, moreover, that (15b, c) can also be written as

$$M_\pm = -cq(\rho_+ \pm \rho_-)^2, \qquad \alpha_\pm = \sqrt{[M_\pm - (1-c^2)q^2]}, \tag{19}$$

where

$$2\rho_\pm = \sqrt{\left[\left(\sqrt{(cq)} \pm \sqrt{\left(\frac{\varepsilon}{h}\right)^2 + \frac{1}{h}}\right]\right.}. \tag{20}$$

This variety in form for $(M_\pm, \alpha_\pm)$ proves convenient in calculations.

Application of (14) to (11) and (12) gives the four conditions

$$\sigma^*_{xy} = 0, \quad u^*_y = V^*_-, \quad \theta^*_{,y} = -F^*, \quad \sigma^*_y = -P\,\mathrm{e}^{qL} + Y^* + \sigma^*_+ \tag{21a–d}$$

along $y = 0^+$ where, more explicitly

$$Y^* = -\frac{Y}{q}(1-\mathrm{e}^{qd}), \qquad F^* = \int_{-d}^{0} F(t)\,\mathrm{e}^{-qt}\,\mathrm{d}t \tag{22}$$

and σ^*_+ exists for $\mathrm{Re}\,(q) > 0^-$ while V^*_- exists for $\mathrm{Re}\,(q) < 0^+$.

Substitution of (15) into (21a–c) eliminates the terms $(A_\pm, B)$ whereupon (21d) produces the single equation

$$\frac{\mu}{m^2\alpha_-} R_T V^*_- = \mu\frac{\beta T}{m^2}\left(\frac{1}{\alpha_+} - \frac{1}{\alpha_-}\right)\frac{F^*}{M_+ - M_-} - P\,\mathrm{e}^{qL} + Y^* + \sigma^*_+ \tag{23}$$

for the unknown functions (V^*_-, σ^*_+). Here

$$c^2q^2(M_+ - M_-)R_T = M_-\alpha_-\left(4q^2b + \frac{T^2}{\alpha_+}\right) - M_+(4q^2b\alpha_- + T^2) = D_T \tag{24}$$

and it can be shown that R_T vanishes at the origin, has the branch cut $\mathrm{Im}\,(q) = 0$, $-q_\varepsilon < \mathrm{Re}\,(q) < 0$ and behaves as

$$c^2q^2R_T \sim R, \quad |q| \to \infty. \tag{25}$$

In light of this behavior and that of α_-, we rearrange (23) as

$$\frac{1}{m^2}\sqrt{\left(-\frac{q}{c}\right)} V^*_- = \frac{q}{\mu R_T}\sqrt{\left[(r_+ - r_-)^2 + \frac{q}{c}\right]}\sigma^*_+ + \Omega \tag{26a}$$

$$\Omega = \frac{1}{R_T}\sqrt{\left[(r_+ - r_-)^2 + \frac{q}{c}\right]}\left[\frac{q}{\mu}(Y^* - P\,\mathrm{e}^{qL}) + \frac{\beta T}{m^2}\left(\frac{1}{\alpha_+} - \frac{1}{\alpha_-}\right)\frac{F^*}{M_+ - M_-}\right]. \tag{26b}$$

The left-hand side of (26a) is analytic for Re $(q) < 0^+$, while the first term on the right-hand side is analytic for Re $(q) > 0^-$. By using the decomposition procedure described by Noble (1958), the function Ω can be written as the sum of terms $\Omega_\pm$ that are also analytic in, respectively, the overlapping half-planes Re $(q) > 0^-$ and Re $(q) < 0^+$. Equation (26a) can then be rewritten as

$$\frac{1}{m^2}\sqrt{\left(-\frac{q}{c}\right)}V_-^* - \Omega_- = \frac{q}{\mu R_T}\sqrt{\left[(r_+ - r_-)^2 + \frac{q}{c}\right]}\sigma_+^* + \Omega_+, \tag{27}$$

where, in light of (22)

$$\frac{\pi}{c^2}\Omega_+ = \frac{1}{\mu}\left[\int_{-\infty}^{-q_c} g_2(v) - \int_{-q_c}^{0} g_1(v)\right]\left[P\,e^{vL} + \frac{Y}{v}(1-e^{vd})\right]\frac{dv}{(v-q)\sqrt{(-cv)}}$$
$$-\beta\int_{-q_c}^{0}\frac{g_{1\beta}(v)}{v-q}\int_{-d}^{0}F(t)\,e^{-vt}\,dt\,\frac{dv}{\sqrt{(-cv)}} \tag{28a}$$

$$\Omega_- = \Omega - \Omega_+. \tag{28b}$$

In (28), (16) still holds, with q replaced by the dummy variable v, and

$$Dg_1(v) = v^3 a_- \alpha_+^2 (M_+ - M_-)[M_+ T^2 - 4v^2|b|a_-(M_+ - M_-)] \tag{29a}$$

$$Dg_{1\beta}(v) = v^3 a_- \alpha_+ T(M_+ - M_-)(4v^2|b|a_- - T^2) \tag{29b}$$

$$D_0 g_2(v) = v^3 a_- a_+ (M_+ - M_-) \tag{29c}$$

$$D = \alpha_+^2[M_+ T^2 - 4v^2|b|a_-(M_+ - M_-)]^2 + (M_- T^2 a_-)^2 \tag{29d}$$

$$D_0 = M_+ a_+(4v^2|b|a_- - T^2) - M_- a_-(4v^2|b|a_+ - T^2) \tag{29e}$$

$$a_\pm = \sqrt{(cv)}\left[(r_+ \pm r_-)^2 + \frac{v}{c}\right], \quad |b| = \sqrt{(1-m^2c^2)}|v|. \tag{29f}$$

The Abelian theorems require that for $y = 0$, $x = 0^-$,

$$V_- \sim \lim_{|q|\to\infty} qV_-^* \tag{30}$$

but (13) implies that the left-hand side of (30) vanishes. Therefore, V_-^* must behave as $O(q^{-1})$, $|q| \to \infty$. A check of each term in Ω_- then shows that the left-hand side of (27) must also vanish when $|q| \to \infty$. Because the two sides of (27) are analytic in overlapping half-planes, each must be an analytic continuation of the same entire function. But the vanishing of the left-hand side as $|q| \to \infty$ implies by Liouville's theorem that the entire function itself must be zero. Therefore, each side of (27) can be solved separately for (σ_+^*, V_-^*).

TRANSFORM INVERSIONS

With (σ_+^*, V_-^*) in hand, elements of the solution field $(\mathbf{u}, \theta)$ can be determined by performing the inversion operation

$$g(x) = \frac{1}{2\pi i}\int_\Gamma g^* e^{qx}\,dq, \tag{31}$$

where the integration path Γ runs, in this instance, always along the entire Im (q)-axis.

Solving the right-hand side of (27) for σ_+^* and then allowing $|q|$ to grow large gives the approximation

$$\sigma_+^* \sim \frac{R}{a}\sqrt{(cgh)}\Omega_0, \tag{32}$$

where, from (18)–(20), (28) and (29), we have

$$\pi\Omega_0 = \left[-\int_0^{c_\varepsilon} g_1(v) + \int_{c_\varepsilon}^{\infty} g_2(v)\right]\left[P\,\mathrm{e}^{-vL'} - \frac{h}{v}Y(1-\mathrm{e}^{-vd'})\right]\frac{\mathrm{d}v}{\sqrt{(cv)}} - \mu\beta\int_0^{c_\varepsilon} g_{1\beta}(v)\int_{-d}^{0} F(t)\,\mathrm{d}^{vt'}\,\mathrm{d}t\frac{\mathrm{d}v}{\sqrt{(cv)}}, \tag{33}$$

where the prime denotes non-dimensionalization with respect to h, the form of (29) is still valid but now v is a dimensionless variable and

$$\alpha_+ = \sqrt{(cv)}\sqrt{\left[(\rho_+ + \rho_-)^2 - \frac{v}{c}\right]}, \qquad a_\pm = \sqrt{(cv)}\sqrt{\left[\frac{v}{c} - (\rho_+ \pm \rho_-)^2\right]} \tag{34a}$$

$$M_\pm = cv[(\rho_+ \pm \rho_-)^2 - cv], \qquad 2\rho_\pm = \sqrt{[(\sqrt{(cv)} \pm 1)^2 + \varepsilon]}. \tag{34b}$$

Substitution of (32) into (31) and using Cauchy theory for $x > 0$ to transform the integration path onto the branch cuts on the negative Re (q)-axis gives an integration that can be carried out exactly to produce the result

$$\sigma_+ \sim \frac{R}{a}\sqrt{\left(\frac{ch}{\pi x}\right)}\Omega_0 \tag{35}$$

which is valid, in view of the Abelian theorems, for $x \sim 0^+$.

The left-hand side of (27) can be solved for V_-^*, the result substituted into (31), and Cauchy theory used for $x < 0$ to transform the integration path onto the branch cuts on the positive Re (q)-axis. The resulting exact expression for V_- when $-d < x < 0$ is

$$\frac{\mu\pi}{hc^2}V_- = \left[-\int_0^{c_\varepsilon} g_1(v) + \int_{c_\varepsilon}^{\infty} g_2(v)\right]S(v)\frac{\mathrm{d}v}{v^2} - Y\int_0^{\infty} g_3(v)(1-\mathrm{e}^{vx'})\,\mathrm{d}v - \mu\beta\int_0^{c_\varepsilon} g_{1\beta}(v)S_\beta(v)\frac{\mathrm{d}v}{v}, \tag{36}$$

where

$$S(v) = vP\,\mathrm{e}^{-v(x'+L')} + hY[\mathrm{e}^{-v(x'+d')} - 1] - [vP\,\mathrm{e}^{-vL'} + hY(\mathrm{e}^{-vd'} - 1)]\,\mathrm{erfc}\,(\sqrt{(-vx')}) \tag{37a}$$

$$S_\beta(v) = \left[\int_{-d}^{x} - \int_{-d}^{0}\mathrm{erfc}\,(\sqrt{(-vx')})\right]F(t)\,\mathrm{e}^{v(t'-x')}\,\mathrm{d}t \tag{37b}$$

$$D_0 g_3(v) = v(M_+ - M_-)a_+ a_-. \tag{37c}$$

In (37c) we devise from (19) and (20) the relations

$$M_\pm = -cv(\rho_+ \pm \rho_-)^2, \quad a_\pm = \sqrt{[(1-c^2)v^2 - M_\pm]}, \quad 2\rho_\pm = \sqrt{[(\sqrt{(cv)} \pm \varepsilon)^2 + 1]}. \tag{38}$$

It can be shown that V_- given by (36) vanishes when $x = 0^-$, as (13) requires.

Finally, knowledge of (σ_+^*, V_-^*) allows, through the quantities $(A_\pm, B)$ eliminated

earlier, an expression for θ^* to be obtained from (15a) as

$$\theta^* = \frac{m^2\varepsilon(cq)^3}{\mu h\beta D_T}\left[Y^* - P\,e^{qL} - \frac{\mu}{\alpha_-}\sqrt{(-cq)}R_T\Omega_+\right]\left(\frac{e^{-\alpha_+ y}}{\alpha_+} - \frac{e^{-\alpha_- y}}{\alpha_-}\right)$$
$$- \frac{F^*}{D_T}\left[M_+\left(4q^2b + \frac{T^2}{\alpha_-}\right)\frac{e^{-\alpha_+ y}}{\alpha_+} - M_-\left(4q^2b + \frac{T^2}{\alpha_+}\right)\frac{e^{-\alpha_- y}}{\alpha_-}\right], \quad (39)$$

where (16)–(18), (22) and (24) hold. Despite its formidable appearance, substitution of (39) into (31) and use of the Cauchy theorem allows the temperature field θ to be derived. For $(x, y) = 0$, this field gives the simple expression

$$\theta = \frac{-\varepsilon K}{2\mu\beta h}\frac{c(a-1)}{R}(Yd - P) - \frac{1}{\pi}\int_{-d}^{0} F(t)\,\ln\left(-\frac{t}{d}\right)dt. \quad (40)$$

The form of (40) indicates that much of the temperature field detail due to the crack/zone vanishes continuously at the inelastic zone edge.

SOLUTION ASPECTS

With (35), (36) and (40) in hand, formulas analogous to (5) and (6) can now be obtained. First of all, the Dugdale (1960) model again precludes the singular behavior exhibited in (35). Therefore, Ω_0 must vanish, which leads to the equation

$$\left[\int_0^{c_\varepsilon} g_1(v) - \int_{c_\varepsilon}^{\infty} g_2(v)\right]\left[P\,e^{-vL'} - Y\frac{h}{v}(1 - e^{-vd'})\right]\frac{dv}{\sqrt{(cv)}}$$
$$- \mu\beta F_0\int_0^{c_\varepsilon} g_{1\beta}(v)\int_{-d}^{0} f(t)\,e^{vt'}\,dt\frac{dv}{\sqrt{(cv)}} = 0, \quad (41)$$

where $F(t)$ has been rewritten as

$$F(t) = F_0 f(t), \quad |f(t)|_{MAX} = 1, \quad -d < t < 0. \quad (42)$$

That is, F_0 is the heat flux amplitude while $f(t)$ gives the details of the flux variation over the inelastic zone.

Upon setting $x = -d$, (36) produces the expression for the COD

$$\frac{\mu\pi}{hc^2}\delta_t = \left[-\int_0^{c_\varepsilon} g_1(v) + \int_{c_\varepsilon}^{\infty} g_2(v)\right]S_d(v)\frac{dv}{v^2}$$
$$- Y\int_0^{\infty} g_3(v)(1 - e^{-vd'})\,dv + \mu\beta\int_0^{c_\varepsilon} g_{1\beta}(v)S_{\beta d}(v)\frac{dv}{v}, \quad (43)$$

where now

$$S_d(v) = vP\,e^{-v(L'-d')} - [vP\,e^{-vL'} + hY(e^{-vd'} - 1)]\,\mathrm{erfc}\,(\sqrt{(vd')}) \quad (44a)$$

$$S_{\beta d}(v) = -F_0\,\mathrm{erfc}\,(\sqrt{(vd')})\int_{-d}^{0} f(t)\,e^{v(t'+d')}\,dt. \quad (44b)$$

It is noted that both (41) and (43) are much more dependent upon the crack propagation rate parameter c than are their non-thermal counterparts.

Finally, the temperature change at the inelastic zone edge follows directly from (40) upon substitution of (42). For experimentally observed values of (δ_t, θ_0), eqns (40)–(43) can be used to relate weighted integrals of $F(t)$ and (d, P) for a given c. For purposes of illustrating such a process, we here choose

$$f(t) = \sin\left(-\pi\frac{t}{d}\right), \quad -d < t < 0 \tag{45}$$

so that only F_0 is needed to determine the flux function and, consequently, specific values of (d, P) can be found for a given c and (δ_t, θ_0). Besides its simplicity, the form (45) imposes flux continuity everywhere along $y = 0$.

This procedure could in principle, of course, be generalized to determine totally the flux $F(t)$ merely by matching the complete temperature change field obtained from (39) to values found experimentally at various points around the crack. However, the special case considered here will be sufficient to, as stated, illustrate the procedure.

The material parameters used for the non-thermal case are again employed, and the thermal properties

$$\varepsilon = 0.01, \quad \beta = -8.2\times10^{-5}/\mathrm{K}, \quad h = 0.00167\,\mu\mathrm{m}, \quad \theta_0 = 300\,\mathrm{K} \tag{46}$$

chosen. The (ε, β, h)-values are consistent with the steel-like nature of the sheet (B), while the θ_0 is typical of values found (Zehnder and Rosakis, 1991) near a steady-state growing crack. The results for d and P are plotted vs c as the solid lines in Figs 2 and 3, respectively. There it is seen that both quantities decay with increasing crack speed—just as in the non-thermal case. Also, the relative efficiency of keeping L small is again exhibited. For a given crack speed (c), however, the inelastic zone sizes d differ noticeably for the thermal case and the non-thermal cases, and the thermal load P is noticeably smaller. That is, accounting for coupled thermoelastic effects alters zone size and decreases the loading required for crack propagation to proceed.

As the results of Zehnder and Rosakis (1991) and Rosakis *et al.* (1992) indicate, the temperature rise near a crack may be different for different crack speeds. However, without at present sufficient data for the complete range of subcritical c, and with the major purpose of the analysis being to ascertain load/zone size sensitivity to coupled thermal effects, only the representative θ_0-value has been used here.

In Table 1, values of the heat flux amplitude F_0 vs crack propagation rate (c) are given. In light of Figs 2 and 3, the direct variation with c seen implies an inverse variation with zone length d. This observation is consistent with the short-time transient analysis of (B), i.e. inelastic zone concentration increases the heat flux. The extremely high values of F_0 indicate just how localized the temperature effects are—an effect noted experimentally (Shockey *et al.*, 1983; Zehnder and Rosakis, 1991). This localization is enhanced here by the vanishingly thin zone, so that the F_0-values are artificially high.

Table 1.

c	F_0 (L = 0.01 m) (K/μm)	F_0 (L = 0.025 m) (K/μm)
0.05	197	295
0.1	399	596
0.15	611	914
0.2	844	1261
0.25	1111	1657
0.3	1439	2143
0.35	1891	2808
0.4	2652	3911

SUMMARY

Steady-state analyses of rapid quasi-brittle fracture generated in both a non-thermal and a fully coupled thermoelastic solid by moving crack surface loads has been performed. A Dugdale (1960) zone model for rudimentary crack-edge inelasticity was adopted, and, in the thermal case, the heat-producing properties of the zone were characterized by an effective heat flux function. Exact analyses using realistic material properties showed that, in both the thermal and non-thermal problems, smaller forces are required to drive the crack and smaller inelastic zones result the more rapidly the crack runs. Moreover, both problems indicated that locating the crack surface loads close to the crack-edge requires smaller loads and produces smaller inelastic zones.

However, for a given propagation rate, the thermal problem required a smaller applied load, and produced a noticeably different inelastic zone. Indeed, the thermal problem solution expressions were generally more sensitive to crack propagation rate.

In the first-step study, a simple continuous function was *a priori* chosen to represent the flux variation over the zone, but the flux amplitude was determined by matching the inelastic zone edge temperature with a value typical of those found in steady-state crack growth. The amplitude varied with zone size in a manner consistent with that calculated for short-time, transient crack propagation. The values were artificially high, due most likely to the vanishingly thin zone model, but were consistent with the rapid fall-off in temperature away from the crack often seen experimentally.

Thus, in summary, these analyses showed that coupled thermoelastic effects triggered by rudimentary inelastic crack-edge zones are important in predicting the loads necessary to drive rapid quasi-brittle fracture. In particular, the relation between load, inelastic zone size and crack propagation rate is stronger than that predicted by a non-thermal study.

Future work will consider steady-state fracture in a finite body, which should allow an even more valid use of experimental data. Temperature fields around the crack will be matched at several points, so that a complete flex function can be determined. Moreover, only those crack speeds that correspond to known temperature fields will be treated.

The strict interpretation of the Dugdale model adopted here precluded the existence of a stress intensity factor. Moreover, while COD-based fracture criteria are often related to fracture toughness (Ewalds and Wanhill, 1985), this first-step analysis chose to focus on the temperature field. Because thermal effects on toughness can be important (Zehnder and Rosakis, 1991), this parameter will be examined in future work, however.

Future work will also relate the flux function obtained to models for plastic work rate in the inelastic zone. As Rice and Levy (1969) showed—at least for an uncoupled elastic solid—crack-edge temperature predictions do depend on the form of the plastic work terms adopted. It is felt, nonetheless, that the heat flux characterization of a rudimentary inelastic zone as a boundary effect on a coupled thermoelastic solid represents an effective, first-step method of studying rapid quasi-brittle fracture, whether transient (B) or, as here, steady-state.

Acknowledgement—This research was carried out with the support of NSF Grant DMS 9121700 and also in part by the NSF/EPSCoR program in Inverse Problems and Quantitiative Non-destructive Evaluation at the University of Kentucky.

REFERENCES

Brock, L. M. (1992a). Transient thermal effects in dynamic quasi-brittle fracture under stress wave loading. In *Advances in Local Fracture/Damage Models of Engineering Problems* (Edited by J. H. Giovanola and A. S. Rosakis), ASME Symposium Volume AMD-137. ASME, New York.

Brock, L. M. (1992b). Transient thermal effects in edge dislocation generation near a crack edge. *Int. J. Solids Structures* **29,** 2217–2234.

Brock, L. M. (1993). Early effects of temperature-dependent yield stress in a transient analysis of fracture. *Acta Mech.* **97,** 101–114.

Brock, L. M., Matic, P. and DeGiorgi, V. G. (1992). Early transient response during crack propagation in a weakly-coupled thermoelastic solid. *Int. J. Solids Structures* **29,** 973–989.

Brock, L. M. and Thomas, J. P. (1992). Thermal effects in rudimentary crack edge inelastic zone growth under stress wave loading. *Acta Mech.* **93,** 223–239.

Chadwick, P. (1960). Thermoelasticity: the dynamical theory. In *Progress in Solids Mechanics* (Edited by I. N. Sneddon and R. Hill). North-Holland, Amsterdam.
Dugdale, D. S. (1960). Yielding of steel sheets containing slits. *J. Mech. Phys. Solids* **8,** 100–104.
Ewalds, H. L. and Wanhill, R. J. H. (1985). *Fracture Mechanics.* DUM/Edward Arnold, Delft/London.
Freund, L. B. (1990). *Dynamic Fracture Mechanics.* Cambridge University Press.
Freund, L. B. and Hutchinson, J. W. (1985). High strain-rate growth in rate-dependent plastic solids. *J. Mech. Phys. Solids* **33,** 169–191.
Noble, B. (1958). *Methods Based on the Wiener–Hopf Technique.* Pergamon Press, New York.
Parvin, M. (1979). Theoretical prediction of temperature rise at a tip of a running crack. *Int. J. Fract.* **8,** 397–404.
Rice, J. R. and Levy, N. (1969). Local heating by plastic deformation at a crack tip. In *Physics of Strength and Plasticity* (Edited by A. S. Argon). MIT Press, Cambridge, MA.
Rosakis, A. J., Mason, J. J. and Ravichandran, G. (1992). The conversion of plastic work to heat around a dynamically propagating crack in metals. SM report 92-17, California Institute of Technology, Pasadena, CA.
Shockey, D. A., Kalthoff, J. F., Klemm, W. and Winkler, S. (1983). Simultaneous measurements of stress intensity factor and toughness for fast-running crack in steel. *Exp. Mech.* **23,** 140–145.
Sneddon, I. N. and Lowengrub, M. (1969). *Crack Problems in the Classical Theory of Elasticity.* John Wiley, New York.
Taylor, G. I. and Quinney, M. A. (1934). The latent energy remaining in a metal after cold working. *Proc. R. Soc.* **A143,** 307–322.
Weichert, R. and Schoenert, K. (1978). Heat generation at the tip of a moving crack. *J. Mech. Phys. Solids* **26,** 151–161.
Yoffe, E. H. (1951). The moving Griffith crack. *Phil. Mag.* **42,** 739–750.
Zehnder, A. T. and Rosakis, A. J. (1991). On the temperature distributions at the vicinity of dynamically propagating cracks in 4340 steel. *J. Mech. Phys. Solids* **39,** 385–415.